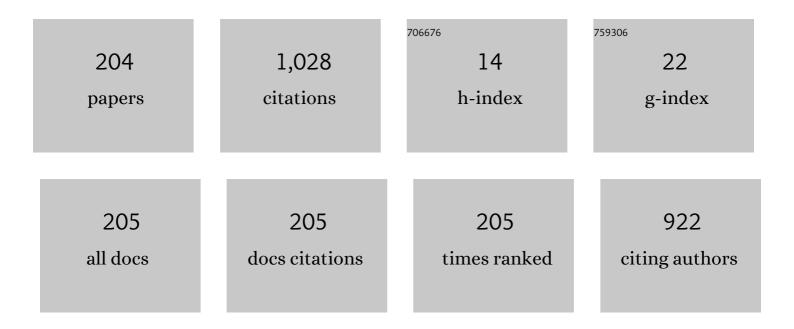
List of Publications by Year in descending order

Source: https://exaly.com/author-pdf/9428351/publications.pdf Version: 2024-02-01



#	Article	IF	CITATIONS
1	Investigation of structural, morphological, and optoelectronic properties of Ga-doped TiO2 nanoparticles for electron transport layer in solar cell applications: An experimental and theoretical study. Journal of Physics and Chemistry of Solids, 2022, 161, 110410.	1.9	2
2	Device Simulation of Ag <sub>2</sub> SrSnS <sub>4</sub> and Ag <sub>2</sub> SrSnSe <sub>4</sub> Based Thinâ€Film Solar Cells from Scratch. Advanced Theory and Simulations, 2022, 5, .	1.3	6
3	Enhanced resonances by waveguide wrapping of a bulbed microring resonator. Applied Optics, 2022, 61, 3279.	0.9	2
4	Determinants Affecting the Performance of CZTSSe: Antisite Defects and Multiple Quantum Confinement for Photon-Sensitive Devices. IEEE Sensors Journal, 2022, 22, 15944-15952.	2.4	6
5	Exploring the effect of Ga3+ doping on structural, electronic and optical properties of CH3NH3PbCl3 perovskites: an experimental study. Journal of Materials Science: Materials in Electronics, 2021, 32, 12841-12855.	1.1	7
6	First-Principles Studies for Electronic Structure and Optical Properties of Strontium Doped β-Ga2O3. Micromachines, 2021, 12, 348.	1.4	18
7	MoS2/h-BN/Graphene Heterostructure and Plasmonic Effect for Self-Powering Photodetector: A Review. Materials, 2021, 14, 1672.	1.3	18
8	First principle study on structural and optoelectronic properties and band-gap modulation in germanium incorporated tin (IV) oxide. Materials Today Communications, 2021, 27, 102393.	0.9	2
9	An ab-initio investigation of mechanical and thermodynamic properties of Ag2MgSn(S/Se)4 in kesterite and stannite phases. Applied Physics A: Materials Science and Processing, 2021, 127, 1.	1.1	5
10	Properties and perspectives of ultrawide bandgap Ga2O3 in optoelectronic applications. Chinese Journal of Physics, 2021, 73, 195-212.	2.0	32
11	ZnO for performance enhancement of surface plasmon resonance biosensor: a review. Materials Research Express, 2020, 7, 012003.	0.8	69
12	Numerical Modelling of MoS <sub>2</sub> /h-BN/graphene photodetector for self-powering application. , 2020, , .		4
13	Minimum leakage current optimization on 22 nm SOI NMOS device with HfO2/WSix/Graphene gate structure using Taguchi method Journal of Physics: Conference Series, 2020, 1502, 012047.	0.3	1
14	Multilayer CVD-Graphene and MoSâ,, Ethanol Sensing and Characterization Using Kretschmann-Based SPR. IEEE Journal of the Electron Devices Society, 2020, 8, 1227-1235.	1.2	16
15	Foreword Special Issue From the Selected Extended Papers Presented at EDTM 2020. IEEE Journal of the Electron Devices Society, 2020, 8, 1105-1110.	1.2	Ο
16	Structural, electronic and optical properties of Ag2MgSn(S/Se)4 quaternary chalcogenides as solar cell absorber layer: An Ab-initio study. Solar Energy, 2020, 209, 206-213.	2.9	16
17	The sensitivity of sensor based on Microring Resonator (MRR) and Surface Plasmon Resonance (SPR) for diabetes monitoring application. IOP Conference Series: Materials Science and Engineering, 2020, 850, 012048.	0.3	1
18	Enhanced Sensitivity of Microring Resonator-Based Sensors Using the Finite Difference Time Domain Method to Detect Glucose Levels for Diabetes Monitoring. Applied Sciences (Switzerland), 2020, 10, 4191.	1.3	5

#	Article	IF	CITATIONS
19	Impact of Sn doping on methylammonium lead chloride perovskite: An experimental study. Journal of Applied Physics, 2020, 127, .	1.1	11
20	CVD-grown Graphene-on-Au characterization and sensing using Kretschmann-based SPR. , 2020, , .		2
21	Robust Design of Bimetallic ZnO Nanofilm SPR Sensor using Taguchi Method. , 2020, , .		0
22	Numerical Simulation of Tunneling Effect in High-Efficiency Perovskite/Silicon Tandem Solar Cell. , 2020, , .		1
23	Multi-response optimization of chromium/gold-based nanofilm Kretschmann-based surface plasmon resonance glucose sensor using finite-difference time-domain and Taguchi method. Nanomaterials and Nanotechnology, 2020, 10, 184798042098211.	1.2	10
24	Silicon on insulator-based microring resonator and Au nanofilm Krestchmann-based surface plasmon resonance glucose sensors for lab-on-a-chip applications. International Journal of Nanotechnology, 2020, 17, 29.	0.1	7
25	FDTD simulation of Kretschmann based Cr-Ag-ITO SPR for refractive index sensor. Materials Today: Proceedings, 2019, 7, 668-674.	0.9	20
26	Influence of ultrathin chromium adhesion layer on different metal thicknesses of SPR-based sensor using FDTD. Materials Today: Proceedings, 2019, 7, 732-737.	0.9	9
27	Facile charge transfer in fibrous PdPt bimetallic nanocube counter electrodes. New Journal of Chemistry, 2019, 43, 11148-11156.	1.4	5
28	Kretschmann based Surface Plasmon Resonance for Sensing in Visible Region. , 2019, , .		9
29	Label-Free Detection of Dissolved Carbon Dioxide Utilizing Multimode Tapered Optical Fiber Coated Zinc Oxide Nanorice. IEEE Access, 2019, 7, 4538-4545.	2.6	13
30	Analytical modeling and simulation of a fully depleted three-gate silicon MESFET on SOI material. Journal of Computational Electronics, 2019, 18, 91.	1.3	2
31	High Sensitivity Au-based Kretschmann Surface Plasmon Resonance Sensor for Urea Detection. Sains Malaysiana, 2019, 48, 1179-1185.	0.3	10
32	Refractive Index and Sensing of Glucose Molarities determined using Au-Cr K-SPR at 670/785 nm Wavelength. Sains Malaysiana, 2019, 48, 1259-1265.	0.3	15
33	A modified two dimensional analytical model for short-channel fully depleted SOI MESFET's. Microelectronics Reliability, 2018, 83, 173-179.	0.9	5
34	Gamma–Radiation-Assisted Synthesis of Luminescent ZnO/Ag Heterostructure Core–Shell Nanocomposites. Plasmonics, 2018, 13, 771-778.	1.8	2
35	Graphene-MoS <inf>2</inf> SPR-based biosensor for urea detection. , 2018, , .		6
36	Modeling of microring resonators for biochemical detection. Materials Today: Proceedings, 2018, 5, 13703-13710.	0.9	3

P SUSTHITHA MENON

#	Article	IF	CITATIONS
37	Detection of Uric Acid Using Kretschmann-based SPR Biosensor with MoS <sub>2</sub> -Graphene. , 2018, , .		2
38	Taguchi optimization of Surface Plasmon Resonance-Kretschmann biosensor using FDTD. , 2018, , .		1
39	Taguchi optimization of Surface Plasmon Resonance-Kretschmann biosensor using FDTD. , 2018, , .		4
40	Urea and creatinine detection on nano-laminated gold thin film using Kretschmann-based surface plasmon resonance biosensor. PLoS ONE, 2018, 13, e0201228.	1.1	57
41	Pengoptimuman Sensor Resonans Plasmon Permukaan berdasarkan Kretschmann dengan Kaedah Taguchi. Sains Malaysiana, 2018, 47, 2565-2571.	0.3	4
42	Graphene-Based Plasmonic Photonic Crystal Waveguide Integrated Biosensor Circuit. Journal of Nanoelectronics and Optoelectronics, 2018, 13, 839-845.	0.1	1
43	Graphene-based surface plasmon resonance urea biosensor using Kretschmann configuration. , 2017, , .		16
44	Investigation of grapheneâ€onâ€metal substrates for SPRâ€based sensor using finiteâ€difference time domain. IET Nanobiotechnology, 2017, 11, 981-986.	1.9	20
45	Investigation of AWG demultiplexer based SOI for CWDM application. EPJ Web of Conferences, 2017, 162, 01035.	0.1	4
46	Urea biosensor utilizing graphene-MoS <inf>2</inf> and Kretschmann-based SPR. , 2017, , .		11
47	Effects of rain attenuation on 28-30CHz bands for beyond 4G terrestrial mobile communications. , 2017, , .		0
48	Influence of electromagnetic (EM) waves polarization modes on surface plasmon resonance. EPJ Web of Conferences, 2017, 162, 01008.	0.1	4
49	Optical interconnect chip with SPR-based photonic crystal waveguide sensor. , 2017, , .		1
50	Implementation of SOA and EDFA Combination in DWDM System. Advanced Science Letters, 2017, 23, 4065-4067.	0.2	1
51	Performance Characterization of Schottky Tunneling Graphene Field Effect Transistor at 60 nm Gate Length. Sains Malaysiana, 2017, 46, 1089-1095.	0.3	2
52	Comparative Performances of SOI-Based Optical Interconnect vs. Electrical Interconnect in Analog Electronic Applications. IEICE Transactions on Electronics, 2017, E100.C, 655-661.	0.3	0
53	Process Parameters Optimization of 14nm MOSFET Using 2-D Analytical Modelling. MATEC Web of Conferences, 2016, 78, 01017.	0.1	0
54	Optical interconnect performances in two stage CMOS buffer. , 2016, , .		0

#	Article	IF	CITATIONS
55	Delay analysis in symmetrical SOI-based rib waveguide for high speed optical interconnect. , 2016, , .		3
56	Large dynamic range operation of ultra-higher number MWFLs affected by MZI-SI. Laser Physics, 2016, 26, 115101.	0.6	0
57	FDTD numerical analysis of SPR sensing using graphene-based photonic crystal. , 2016, , .		8
58	Copper-graphene SPR-based biosensor for urea detection. , 2016, , .		20
59	Investigation on electrical conductivity of strontium (Sr <sup>2+</sup> ) influenced CaTi <inf>0.8</inf> Fe <inf>0.2</inf> O <inf>3</inf> polycrystalline perovskite. , 2016, , .		3
60	Scattering of waves by chiral medium-coated dielectric elliptical/circular cylinders with PEC sheath helix loading. Journal of Electromagnetic Waves and Applications, 2016, 30, 1504-1518.	1.0	3
61	Process Characterization of 32nm Semi Analytical Bilayer Graphene-based MOSFET. MATEC Web of Conferences, 2016, 78, 01016.	0.1	2
62	Recent Advances in Shape-Controlled Synthesis of Noble Metal Nanoparticles by Radiolysis Route. Nanoscale Research Letters, 2016, 11, 287.	3.1	56
63	Radiolytic formation of highly luminescent triangular Ag nanocolloids. Journal of Radioanalytical and Nuclear Chemistry, 2016, 307, 985-991.	0.7	9
64	Study of the side gate junctionless transistor in accumulation region. Microelectronics International, 2016, 33, 61-67.	0.4	2
65	FDTD analysis of structured metallic nanohole films for LSPR-based biosensor. , 2015, , .		16
66	Observation and comparison of multiwavelength generation erbium doped fibre ring laser utilising photonic crystal fibre with zero dispersion at 1040 nm and 1550 nm. IEICE Electronics Express, 2015, 12, 20150413-20150413.	0.3	0
67	Design and application of 8-channel SOI-based AWG demultiplexer for CWDM-system. AIP Conference Proceedings, 2015, , .	0.3	0
68	Development of process parameters for 22 nm PMOS using 2-D analytical modeling. AIP Conference Proceedings, 2015, , .	0.3	1
69	Comparison of CMOS rectifiers for micropower energy harvesters. , 2015, , .		13
70	On the performance of Mach-Zehnder-Interferometer (MZI) optical modulator on silicon-on-insulator (SOI). , 2015, , .		1
71	Scattering from silver metal cylinder due to L-nihility coated with conducting sheath helix embedded dielectric medium. Journal of Electromagnetic Waves and Applications, 2015, 29, 1354-1374.	1.0	14
72	Statistical optimization of process parameters for threshold voltage in 22 nm p-Type MOSFET using Taguchi method. , 2015, , .		0

#	Article	IF	CITATIONS
73	4-Channel double S-shaped AWG demultiplexer on SOI for CWDM. , 2015, , .		0
74	Performance on optical properties of AWG based on SOI demultiplexer and receiver sensitivity in CWDM system. , 2015, , .		0
75	Sensitivity improvement of multipath optical ring resonators using silicon-on-insulator technology. , 2015, , .		4
76	Investigation on Optical Interconnect(OI) link performance using external modulator. , 2015, , .		2
77	Characterization of optical coupling loss for AWG demultiplexer on SOI using butt-coupling method. , 2015, , .		0
78	FDTD Analysis on Geometrical Parameters of Bimetallic Localized Surface Plasmon Resonance-Based Sensor. , 2015, , .		10
79	Design of optical single mode splitter using ion exchange method for ammonia biosensor. , 2015, , .		1
80	Twenty two flattened channels L band multi-wavelength erbium doped fiber laser with composite ring cavity. Laser Physics, 2015, 25, 115102.	0.6	1
81	Fabrication of gold strip thin film on glass substrate for plasmonic demodulation application. , 2015, ,		0
82	An assessment study of absorption effect: LED vs tungsten halogen lamp for noninvasive glucose detection. Journal of Innovative Optical Health Sciences, 2015, 08, 1550013.	0.5	9
83	Fe x Ni(1â^'x)OOH hollow-structured nanoparticles formed via γ-radiation induced self-template method. Journal of Radioanalytical and Nuclear Chemistry, 2015, 304, 1339-1343.	0.7	1
84	Structural phase transformations in radiolytically synthesized Al–Cu bimetallic nanoparticles. Journal of Materials Science, 2015, 50, 4348-4356.	1.7	3
85	16-channel arrayed waveguide grating (AWG) demultiplexer design on SOI wafer for application in CWDM-PON. Proceedings of SPIE, 2015, , .	0.8	3
86	The generation of a lower threshold multiwavelength fiber laser in the L-band region assisted by a Sagnac loop mirror. Laser Physics, 2015, 25, 045107.	0.6	0
87	Measurement of nonlinear refractive index based on multiple configuration of FBG in generating multi wavelength. , 2015, , .		0
88	Measurement of a post-amplified CWDM system performance with EDFA-SOA amplifiers. , 2015, , .		1
89	Simple, Easy-use and Low-cost Software for Design of Single and Cascaded Microring Resonators Using Semi-numerical Method. Telkomnika (Telecommunication Computing Electronics and Control), 2015, 13, 820.	0.6	0
90	Optimisation of Process Parameters for Lower Leakage Current in 22 nm n-type MOSFET Device using Taguchi Method. Jurnal Teknologi (Sciences and Engineering), 2014, 68, .	0.3	1

#	Article	IF	CITATIONS
91	Analysis of Jitter Impact on High Speed Transmissions of Wavelength-Division Multiplexing Networks. American Journal of Applied Sciences, 2014, 11, 2016-2020.	0.1	0
92	Design of optical Mach-Zehnder interferometer using ion exchange method for biosensing. , 2014, , .		5
93	Optical loss analysis in 13-channel SOI-based AWG for CWDM network. Journal of Nonlinear Optical Physics and Materials, 2014, 23, 1450008.	1.1	7
94	Design and optimization of a Mach-Zehnder Interferometer (MZI) for optical modulators. , 2014, , .		1
95	Gain performance of cascaded and hybrid semiconductor optical amplifier in CWDM system. Journal of Nonlinear Optical Physics and Materials, 2014, 23, 1450007.	1.1	3
96	Analysis of difference light sources for non-invasive aqueous glucose detection. , 2014, , .		1
97	Electro-optics interaction imaging in active plasmonic devices. Optical Materials Express, 2014, 4, 424.	1.6	19
98	Statistical process modelling for 32nm high-K/metal gate PMOS device. , 2014, , .		4
99	Balance and imbalance of nonlinear optical loop mirror for the realization of multi-wavelength erbium-doped fiber laser. , 2014, , .		Ο
100	Analyses for various doping structures of SOI-based optical phase modulator using free carrier dispersion effect. Optik, 2014, 125, 1800-1803.	1.4	3
101	Effect of process parameter variability on the threshold voltage of downscaled 22nm PMOS using taguchi method. , 2014, , .		Ο
102	Effect of Halo structure variations on the threshold voltage of a 22nm gate length NMOS transistor. Materials Science in Semiconductor Processing, 2014, 17, 155-161.	1.9	12
103	Nonlinear refractive index on multiwavelength generation through mismatch photonic crystal fibre from transmission wavelength. , 2014, , .		0
104	Optimal design of linear tapered double S-shaped arrayed waveguide grating for broad channel spacing on silicon-on-insulator. Optical Engineering, 2014, 53, 087110.	0.5	4
105	Wide Wavelength Range and High Speed SiGe/Si Multi Quantum-Well Silicon-On-Insulator-Based Lateral PIN Photodiode. Journal of Nanoelectronics and Optoelectronics, 2014, 9, 507-510.	0.1	0
106	Application of statistical method to investigate the effects of design parameters on the performance of microring resonator channel dropping filter. International Journal of Numerical Modelling: Electronic Networks, Devices and Fields, 2013, 26, 670-679.	1.2	9
107	Responsivity optimization of a MQW SOI-based lateral PIN photodiode using Taguchi's L <inf>27</inf> orthogonal array. , 2013, , .		5
108	Threshold voltage optimization in a 22nm High-k/Salicide PMOS device. , 2013, , .		4

#	Article	IF	CITATIONS
109	Performance evaluation of 8 channel CWDM system with cascaded SOAs. , 2013, , .		3
110	Development of rain attenuation model for Southeast Asia equatorial climate. IET Communications, 2013, 7, 1008-1014.	1.5	8
111	High performance silicon lateral PIN photodiode. IOP Conference Series: Earth and Environmental Science, 2013, 16, 012032.	0.2	3
112	Absorption Characteristics of Ruthenium (Ru)-II Nanoparticles as a Dissolved Oxygen Sensing Material. Materials Science Forum, 2013, 756, 246-250.	0.3	4
113	12-channel tapered SOI-based AWG for CWDM system. , 2013, , .		6
114	Design and Optimization of 22 nm Gate Length High-k/Metal gate NMOS Transistor. Journal of Physics: Conference Series, 2013, 431, 012026.	0.3	11
115	Numerical investigation of channel width variation in junctionless transistors performance. , 2013, , .		1
116	Flat gain, wide bandwidth of in-line semiconductor optical amplifier in CWDM Systems. IETE Technical Review (Institution of Electronics and Telecommunication Engineers, India), 2013, 30, 516.	2.1	8
117	NANOCRYSTALLINE ALUMINUM DOPED ZINC OXIDE COATED FIBER OPTIC FOR ULTRAVIOLET DETECTION. Journal of Nonlinear Optical Physics and Materials, 2013, 22, 1350037.	1.1	7
118	Angle Shifting in Surface Plasmon Resonance: Experimental and Theoretical Verification. Journal of Physics: Conference Series, 2013, 431, 012028.	0.3	20
119	C-band amplification through fibre ring laser in generating multi wavelength. Proceedings of SPIE, 2013, , .	0.8	1
120	Gold Nanoparticles Grown Using Modified Seed-Mediated Growth Technique. Advanced Science Letters, 2013, 19, 1412-1415.	0.2	4
121	An Ultraviolet Detector Based on Al-Doped ZnO Thin Films Prepared by Sol–Gel Method. Advanced Science Letters, 2013, 19, 1349-1352.	0.2	1
122	Al-Doped ZnO Coated Fiber Optic for Ultraviolet and Acetone Sensing. Advanced Science Letters, 2013, 19, 1306-1309.	0.2	2
123	Design Parameters Investigation of Single Mode Silicon-on-Insulator (SOI) Microring Channel Dropping Filter. Advanced Science Letters, 2013, 19, 199-202.	0.2	2
124	Influences of Light Coupling Techniques to the Excitation of Surface Plasmon Polaritons. Advanced Science Letters, 2013, 19, 66-69.	0.2	12
125	Effects of Ultraviolet Illumination on Sol–Gel Synthesized Al-Doped ZnO Thin Films. Advanced Science Letters, 2013, 19, 816-819.	0.2	2
126	Analysis of Simple Successive Interference Cancellation Scheme in Optical CDMA Spectral Amplitude Coding. Advanced Science Letters, 2013, 19, 190-193.	0.2	0

8

#	Article	IF	CITATIONS
127	Hybrid Wavelength-Division Multiplexing/Optical Code-Division Multiple-Access System Based on Hybrid Spectral/Spatial Coding Scheme. Advanced Science Letters, 2013, 19, 90-94.	0.2	0
128	Optimizing the Modulation Efficiency of Silicon-on-Insulator-Based Optical Phase Modulator. Advanced Science Letters, 2013, 19, 543-546.	0.2	0
129	Performance Optimization of Optical <i>Y</i> -Junction on Silicon-on-Insulator for Mach-Zehnder Interferometer Applications. Advanced Science Letters, 2013, 19, 587-590.	0.2	0
130	Various Sloped Wall Effect on Silicon on Insulator (SOI) Phase Modulator. Advanced Science Letters, 2013, 19, 1438-1440.	0.2	0
131	Effect of Design Parameter Variations on the Quality Factor of a Microring Resonator Filter. Advanced Science Letters, 2013, 19, 1398-1401.	0.2	0
132	Phase Modulation Optimization of Optical Modulator Based on Free Carrier Injection Effect. Advanced Science Letters, 2013, 19, 1471-1474.	0.2	0
133	Dextrose Detection Using Polymer Optical Fiber (POF). Advanced Science Letters, 2013, 19, 1255-1259.	0.2	0
134	Microfabricated Fiber Probe by Combination of Electric Arc Discharge and Chemical Etching Techniques. Advanced Materials Research, 2012, 462, 38-41.	0.3	6
135	DESIGN AND CHARACTERIZATION OF MULTIPLE COUPLED MICRORING BASED WAVELENGTH DEMULTIPLEXER IN SILICON–ON–INSULATOR (SOI). Journal of Nonlinear Optical Physics and Materials, 2012, 21, 1250004.	1.1	6
136	Free Carrier Absorption Loss of Optical Phase Modulator. Advanced Materials Research, 2012, 545, 355-358.	0.3	0
137	Optimization of process parameter variation in 45nm p-channel MOSFET using L <inf>18</inf> orthogonal array. , 2012, , .		3
138	Performance of 18 channel CWDM system with inline Semiconductor Optical Amplifier. , 2012, , .		8
139	NEAR FIELD AND FAR FIELD EFFECTS IN THE TAGUCHI-OPTIMIZED DESIGN OF AN InP/GaAs-BASED DOUBLE WAFER-FUSED MQW LONG-WAVELENGTH VERTICAL-CAVITY SURFACE-EMITTING LASER. Journal of Nonlinear Optical Physics and Materials, 2012, 21, 1250006.	1.1	2
140	Performance of the Active Microring Resonator Based on SOI Rib Waveguide. Advanced Materials Research, 2012, 462, 375-379.	0.3	0
141	Modeling of SOI-based MRR by coupled mode theory using lateral coupling configuration. , 2012, , .		1
142	Performance analysis of multi-weight 2D-OCDMA TEDW. , 2012, , .		2
143	Design study of integrated optical transducer for bioparticles detection. , 2012, , .		2

Scaling down of the 32 nm to 22 nm gate length NMOS transistor. , 2012, , .

9

P SUSTHITHA MENON

#	Article	IF	CITATIONS
145	High performance of a SOI-based lateral PIN photodiode using SiGe/Si multilayer quantum well. , 2012, ,		3
146	Simulation of MQC code for optical CDMA PON system. , 2012, , .		3
147	EFFECT OF LOW TEMPERATURE ON THE FABRICATION OF MICRORING RESONATOR BY WET ETCHING. American Journal of Applied Sciences, 2012, 9, 1922-1928.	0.1	Ο
148	Optical Code-Division Multiple-Access and Wavelength Division Multiplexing: Hybrid Scheme Review. Journal of Computer Science, 2012, 8, 1718-1729.	0.5	14
149	Realization of 2-D OCDMA network using EDW code. Optik, 2012, 123, 1385-1389.	1.4	10
150	Code development for simultaneous in-band transmission of both S AC-Optical CDMA and WDM channels. , 2011, , .		0
151	Performance analysis of SAC/Optical CDMA and WDM under a hybrid overlay scheme. , 2011, , .		1
152	Impact of coupled resonator geometry on silicon-on insulator wavelength filter characteristics. , 2011, , .		3
153	Effects of Mn doping concentrations on properties of ZnO thin films. , 2011, , .		Ο
154	Electrical characteristics of silicon-on-insulator (SOI) phase modulator. , 2011, , .		0
155	Modified ITU-R rain attenuation model for equatorial climate. , 2011, , .		16
156	Concentrationâ€dependent minority carrier lifetime in an In <sub>0.53</sub> Ga <sub>0.47</sub> As interdigitated lateral PIN photodiode model based on spinâ€on chemical fabrication methodology. International Journal of Numerical Modelling: Electronic Networks, Devices and Fields, 2011, 24, 465-477.	1.2	12
157	Transient performance of Silicon-On-Insulator (SOI) Phase Modulator. , 2011, , .		0
158	Electro-Optical Modulator Performance in SOI. , 2011, , .		0
159	Simulation of MQC code of SAC/Optical CDMA and WDM hybrid overlay system. , 2011, , .		2
160	A new analytical model for lateral breakdown voltage of double-gate power MOSFETs. , 2011, , .		2
161	Effect of Taper Angle of the Optical Fiber Microprobe in Power Collection. Advanced Materials Research, 2011, 403-408, 3387-3391.	0.3	4
162	Structural and Optical Properties of Nanostructured Zn <sub>1-X</sub> Mn <sub>x</sub> O Thin Films. Advanced Materials Research, 2011, 378-379, 731-734.	0.3	0

#	Article	IF	CITATIONS
163	Plasma Dispersion Effect for Various Doping Configuration on the SOI Phase Modulator with Trapezoidal Rib Waveguide. Advanced Materials Research, 2011, 403-408, 4403-4407.	0.3	0
164	Performance of Optical Wavelength Demultiplexer Based on Silicon-on-Insulator (SOI) Microring Resonators (MRRs). Advanced Materials Research, 2011, 378-379, 549-552.	0.3	0
165	Study of Fraunhofer Diffraction Pattern from a Circular Aperture Using an Optical Fiber Microprobe. Advanced Materials Research, 2011, 378-379, 565-568.	0.3	Ο
166	Investigation of in-band transmission of both spectral amplitude coding/optical code division multiple-access and wavelength division multiplexingÂsignals. Optical Engineering, 2011, 50, 065001.	0.5	1
167	Process Modeling, Optimization and Characterization of Silicon <100> Optical Waveguides by Anisotropic Wet Etching. Advanced Materials Research, 2011, 403-408, 4295-4299.	0.3	1
168	Active SOI Optical Ring Resonator Based on Free Carrier Injection. Advanced Materials Research, 2011, 403-408, 758-761.	0.3	0
169	Free Carrier Absorption Loss of p-i-n Silicon-On-Insulator (SOI) Phase Modulator. , 2011, , .		3
170	2x2 Optical Switch Based on Silicon-on-Insulator Microring Resonator. Advanced Materials Research, 2011, 378-379, 531-534.	0.3	0
171	InP-based multi-quantum-well mole fraction variation effects on a double wafer-fused GaAs/InP LW-VCSEL. Scientific Research and Essays, 2011, 6, .	0.1	0
172	Effect Of Doping Concentrations On The Properties Of Mn-doped ZnO Nanostructured Thin Films. , 2010, , .		1
173	Long-wavelength MQW Vertical-cavity Surface Emitting Laser: Effects of Lattice Temperature. Journal of Optical Communications, 2010, 31, .	4.0	5
174	Electro-optical modulator performance in SOI. , 2010, , .		1
175	Transient performance of silicon-on-insulator (SOI) phase modulator. , 2010, , .		2
176	VARIATION OF MQW DESIGN PARAMETERS IN A GaAs/InP-BASED LW-VCSEL AND ITS EFFECTS ON THE SPECTRAL LINEWIDTH. Journal of Nonlinear Optical Physics and Materials, 2010, 19, 209-217.	1.1	4
177	Effect of Mn doping on the structural and optical properties of ZnO films. , 2010, , .		3
178	Hybrid SAC/Optical CDMA-WDM overlay system for enhancing network security. , 2010, , .		4
179	Effect of Annealing Temperature on the Structural and Optical Properties of Zn[sub 1â^'x]Mn[sub x]O. , 2010, , .		0
180	Modeling And Analysis Of Lateral Doping Region Translation Variation On Optical Modulator Performance. AIP Conference Proceedings, 2010, , .	0.3	9

#	Article	IF	CITATIONS
181	Operation mode of phase modulation based on carrier dispersion effect in p-i-n diode of silicon rib waveguide. , 2010, , .		0
182	An analysis of silicon waveguide phase modulation efficiency based on carrier depletion effect. , 2010, , .		10
183	Peak power and wavelength optimization of a double-fused LW-VCSEL. , 2010, , .		2
184	Fabrication of optical fiber microprobe using electric arc heating and one-sided pulling technique. , 2010, , .		3
185	Tuning the bandgap of Zn <inf>1−x</inf> Mn <inf>x</inf> O thin films prepared by the sol-gel method. , 2010, , .		1
186	Free carrier absorption loss on p-i-n and n-p-n silicon phase modulator at λ=1.3µm and λ=1.55µm. , 2010, , .		0
187	Effect of MQW design parameters on the characteristics of an air-post 1.5 μm VCSEL. , 2009, , .		0
188	Self-Heating Effects in a Gain-Guided Vertical-Cavity Surface-Emitting Laser. , 2009, , .		1
189	Effect of illumination positioning on the characteristics of an In <inf>0.53</inf> Ga <inf>0.47</inf> as interdigitated lateral PIN photodiode. , 2008, ,		0
190	Design and modeling of a vertical-cavity surface-emitting laser (VCSEL). , 2008, , .		5
191	SNR prediction model of an In <inf>0.53</inf> Ga <inf>0.47</inf> As interdigitated lateral p-i-n photodiode. , 2008, , .		2
192	Concentration and temperature-dependent low-field mobility model for In0.53Ga0.47As interdigitated lateral pin PD. IEICE Electronics Express, 2008, 5, 303-309.	0.3	17
193	An interdigitated diffusion-based In 0.53 Ga 0.47 As lateral PIN photodiode. Proceedings of SPIE, 2007, , .	0.8	4
194	Novel 3D modeling of In 0.53 Ga 0.47 As lateral PIN photodiode. Proceedings of SPIE, 2007, , .	0.8	0
195	Numerical Modeling of a Diffusion-Based In <sub>0.53</sub> Ga <sub>0.47</sub> As Lateral PIN Photodiode for 10 Gbit/s Optical Communication Systems. , 2006, , .		2
196	Surface versus lateral illumination effects on an interdigitated Si planar PIN photodiode. , 2005, , .		2
197	Ultraviolet Sensing by Al-Doped ZnO Thin Films. Advanced Materials Research, 0, 364, 154-158.	0.3	0
198	Influence of Doping Concentrations of Sol Gel Derived Zn <sub>1-x</sub> Mn <sub>x</sub> O Thin Films. Advanced Materials Research, 0, 403-408, 753-757.	0.3	0

#	Article	IF	CITATIONS
199	Analysis of Silicon-On-Insulator (SOI) Buried Waveguide Phase Modulator. Advanced Materials Research, 0, 462, 532-535.	0.3	0
200	Application of Taguchi Method in Designing a 22nm High-k/Metal Gate NMOS Transistor. Advanced Materials Research, 0, 925, 514-518.	0.3	0
201	Taguchi Optimization of a SiGe/Si Quantum Dot SOI-Based Lateral PIN Photodiode. Advanced Materials Research, 0, 925, 646-650.	0.3	0
202	Analysis of Threshold Voltage Variance in 45nm N-Channel Device Using L <sub>27</sub> Orthogonal Array Method. Advanced Materials Research, 0, 903, 297-302.	0.3	4
203	Link Power Level Improvements in an Amplified 8-Channel CWDM System with Hybrid EDFA-SOA Pre-Amplifier. Applied Mechanics and Materials, 0, 799-800, 1361-1365.	0.2	0
204	FDTD Analysis on Geometrical Parameters of Bimetallic Localized Surface Plasmon Resonance-Based Sensor and Detection of Alcohol in Water. International Journal of Simulation: Systems, Science and Technology, 0, , .	0.0	4